European Polymer Journal 134 (2020) 109851

Contents lists available at ScienceDirect

European Polymer Journal

journal homepage: www.elsevier.com/locate/europolj

Updating radical ring-opening polymerisation of cyclic ketene acetals from synthesis to degradation

Jenny Folini[a,1], Wigdan Murad[a,1], Fabian Mehner[b], Wolfgang Meier[a], Jens Gaitzsch[a,b,*]

[a] Department of Chemistry, University of Basel, Mattenstrasse 24a, BPR1096, 4058 Basel, Basel-Stadt, Switzerland
[b] Leibniz-Institut für Polymerforschung Dresden e.V., Hohe Strasse 6, 01069 Dresden, Germany

ARTICLE INFO

Keywords:
RROP
Polyesters
Biodegradation
CKAs
Nanoparticles

ABSTRACT

Radical ring-opening polymerisation (RROP) of cyclic ketene acetals (CKAs) has gained momentum as it yields polyesters as biodegradable polymers from a radical polymerisation. In order to advance the polymerisation, some of its major limitations were addressed in the research presented, focussing on the four mainly used CKAs in modern research on RROP. Monomer synthesis has been updated towards a cobalt/TMSCl-based system that was performed reliably on several monomers at room temperature. Calculations using the density functional theory (DFT) revealed that the ring-opening step is energetically hampered in comparison to a ring-retaining reaction, which explained the challenges faced to promote the ring-opening reaction. Higher molecular weights up to four times the values reached by thermally initiated polymerisation were obtained by exploiting UV light and ultrasound as alternative methods to facilitate the polymerisation. The reaction procedure also influenced thermal properties of the polymers, which in turn affected the enzymatic degradation of nanoparticles based on those polymers. Altogether, the present study offers a holistic update to enhance the RROP of CKAs.

1. Introduction

The continuous development of biodegradable polymers such as polyesters is of significant interest in modern polymer chemistry [1,2]. Ionic ring-opening polymerisation (ROP), polycondensation (PCo) and polyaddition (PAd) are already well-established methods to generate biodegradable polyesters [3,4]. However, all of these methods have limitations either in the range of possible polymers or in the control of the polymerisation. An alternative approach to generate polyesters is radical ring-opening polymerisation (RROP) from cyclic ketene acetals (CKAs) [5,6], which is a chain-growth polymerisation reaching structurally different polyesters than ROP, PCo and PAd. Although RROP has been known for more than 35 years, it has only grasped increased attention over the past decade [5,7–9]. It adheres to three principles of green chemistry [10], since starting diols like 1,4-butanediol and diethylene glycol can be bio-sourced (principle 7), no protection groups are used in monomer synthesis and polymerisation (principle 8) and the resulting polyesters are designed for degradation (principle 10). Recent advances in RROP have seen a surge in available monomers for RROP, increasing the variety of available polymers [5,6]. Polyesters from RROP have been applied as homopolymers [11–14], (block-) copolymers [9,14–17] and also statistic copolymers with vinylic monomers, allowing for the introduction of degradable units in the vinylic main chain [18–23]. Copolymerisation of vinylenes with CKAs can be used for polymerisation-induced self-assembly (PISA) of nanoparticles, which eventually degrade into residual oligomers [24].

A vast majority of reports deploy a similar synthetic strategy to synthesise CKAs (the monomers) *via* a cyclic chlorinated acetal intermediate (acetal route). We have recently introduced a catalytic system based on $CoCl_2$ to synthesise the chlorinated acetal intermediate of the CKA 4,7-dimethyl-2-methylene-1,3-dioxepane (DMMDO) in a more efficient manner (new acetal route). The same study also introduced a new route to reach DMMDO *via* a carbonate intermediate (carbonate route) [14]. The latter pathway then unlocked pH-sensitive CKAs, which led to pH-sensitive biodegradable polyesters from RROP [16]. However, both pathways still require optimisation. It is, for example, unknown how versatile or limited these new synthetic strategies are. Their evaluation and optimisation will be one focus in this work (Fig. 1a).

RROP of CKAs is known to lead to a mixture of repeating units in the final polymer, since an intermediate radical can also propagate chain extension instead of ring-opening. This side reaction leads to repeating

* Corresponding author at: Department of Chemistry, University of Basel, Mattenstrasse 24a, BPR1096, 4058 Basel, Basel-Stadt, Switzerland. Leibniz-Institut für Polymerforschung Dresden e.V., Hohe Strasse 6, 01069 Dresden, Germany.
E-mail address: gaitzsch@ipfdd.de (J. Gaitzsch).
[1] Both authors contributed equally.

https://doi.org/10.1016/j.eurpolymj.2020.109851
Received 7 April 2020; Received in revised form 11 June 2020; Accepted 12 June 2020
Available online 17 June 2020

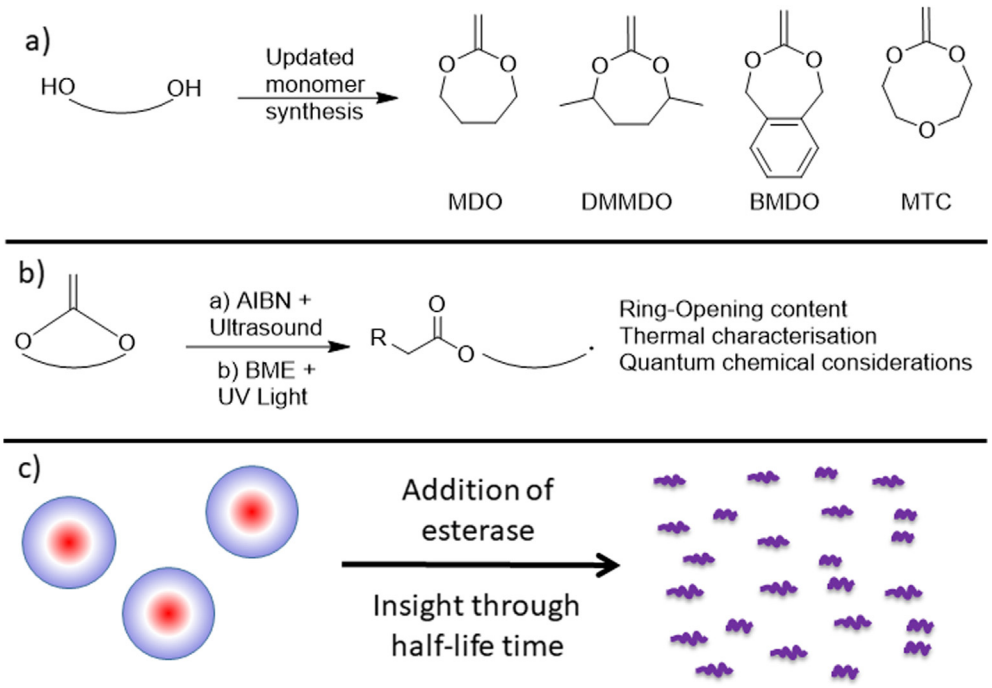

Fig. 1. a) A variety of CKAs were produced using an updated cobalt-catalysed acetal pathway and a new carbonate pathway. b) The CKAs were polymerised using ultrasound-aided polymerisation (US-RROP) as well as UV-assisted polymerisation (photo-RROP) (AIBN = azobis(isobutyronitril); BME = benzoin methyl ether). c) These polymers were then used in amphiphilic block copolymers that self-assembled into nanoparticles, which will allow for addressing details of their biodegradation behaviour.

units that are not biodegradable [5]. In addition to this major side reaction, very few studies report on the challenges faced during the synthesis of homopolyesters from RROP with molecular weights above 5–10 kg/mol [23,25]. Both limitations are currently overcome by co-polymerisation with vinylic monomers [17,26], but have not been solved for homopolyesters. The work presented here investigates a possible explanation for the limitations using calculations based on density functional theory (DFT). In order to overcome those limitations, initial studies into alternative synthetic approaches are addressed as well. (Fig. 1b).

One of the most promising applications of RROP is their use in amphiphilic block copolymers, which undergo self-assembly into biodegradable nanoparticles. Degradation of such nanoparticles can be triggered by the addition of esterase (Fig. 1c) [14,16]. The final goal of this work was to compare different polyesters from RROP and to evaluate their suitability for self-assembly applications, based on their ability to form nanoparticles and their degradation times upon adding esterase. Results from different experiments are then linked to gain a deeper insight into polyesters from RROP.

2. Materials and methods

2.1. Materials

Unless stated otherwise, all chemicals were used as received. Diethylene glycol, 2,5-hexanediol, 1,4-butanediol, 1,2-benzenedimethanol, cobalt(II) chloride ($CoCl_2$), potassium *tert*-butoxide (KO^tBu), trimethylchlorosilane (TMSCl), *tert*-butanol (^tBuOH), methyl-capped poly(ethylene glycol) (MW = 550 g/mol), ethyl chloroformate, titanocene dichloride, benzoin methyl ether (BME), azobisisobutyronitrile (AIBN), 3 M methylmagnesium chloride (MeMgCl) in THF, dry tetrahydrofuran (THF), DOWEX 50WX2 and DOWEX 50WX80 were purchased from *Sigma-Aldrich*. Dimethylformamide (DMF), petrol ether (PE with a boiling point of 60 °C), methanol (MeOH), ethanol (EtOH), dichloromethane (DCM), toluene (PhMe), ethyl acetate (EtOAc), were purchased from *Biosolve* (Biosolve Chimie SARL, France). Acetonitrile (MeCN), sodium chloride (NaCl), sodium hydrogen carbonate ($NaHCO_3$), magnesium sulfate ($MgSO_4$), ammonium chloride (NH_4Cl) (technical grade) were purchased from *ThermoFisher Scientific*.

3. Methods

Gel Permeation Chromatography (GPC) was performed on an *Agilent infinity 1200* instrument (Polymer Standard Services, Germany) with chloroform as eluent and two Mixed-C columns (Polymer Standards Services, Germany) were used for separation. The column oven was set to 35 °C and a flow rate of 1.0 mL/min applied. All GPC traces shown were recorded using a refractive index (RI) detector.

All *NMR* experiments were performed on a *Bruker Avance III* NMR spectrometer operating at 500 MHz proton frequency and at 125 MHz for spectra of ^{13}C. The instrument was equipped with a direct observe 5-mm BBFO smart probe. The experiments were performed at 298 K and the temperature was calibrated using a methanol standard showing accuracy within ± 0.2 K. The spectra for all monomers can be found in section 2 of the supporting information (SI).

Dynamic Light Scattering (DLS) was performed on a LS spectrometer from *LS Instruments* (Switzerland) with a HeNe laser (633 nm) with varying scattering angles. A scattering angle of 90° was used for all and the device was set to give the data in intensity-mode. To monitor particle degradation, the laser intensity was set to 3.5% and the detector count rate averaged over 3 measurements of 10 s each.

Differential scanning calorimetry (DSC) was conducted on a *DSC 214 Polyma* (Netzsch GmbH, Austria) under a nitrogen atmosphere from −120 to 190 °C with a heating rate of 10 $K{\cdot}min^{-1}$ and cooling rate of 20 $K{\cdot}min^{-1}$. Samples were first heated to 190 °C (first heating) before being cooled down (first cooling). The DSC curves shown correspond to the first cooling and the second heating curve.

3.1. Synthetic procedures:

2-methylene-1,3-dioxepane (MDO) via an acetal intermediate:

Step 1: 1,4-Butanediol (10.0 g, 111 mmol, 1.0 eq.) and $CoCl_2$ (varying amounts, see main paper for details) were dissolved in dry MeCN (840 mL). TMSCl (12.2 g, 112 mmol, 1.01 eq.) and 2-chloro-1,1-dimethoxyethane (13.9 g, 112 mmol, 1.01 eq.) were added consecutively. The mixture was left stirring overnight at RT. The mixture was added to water (450 mL) and extracted with EtOAc (3 × 800 mL). The combined organic phase was washed with sat.

$NaHCO_3$ (400 mL) solution, dried over Na_2SO_4 and filtered. The solvent was removed under reduced pressure. The product was further purified by distillation (boiling point (b.p.) 62 °C / 10 mbar) to give the chlorinated acetal (10.0 g, 66.4 mmol, 60%) as a colourless liquid. ^{1}H NMR (500 MHz, $CDCl_3$, δ/ppm): 1.61–1.74 (m, 4H, $-CH_2-CH_2-$), 3.41 (d, 2H, CH_2-Cl), 3.60–3.68 (m, 2H, $-OCH_2$), 3.87–3.96 (m, 2H, $-OCH_2$), 4.87 (t, 1H, OCHO).

Step 2: The acetal just obtained (10.0 g, 66.5 mmol, 1.0 eq.) and KO^tBu (8.90 g, 79.8 mmol, 1.2 eq.) were dissolved in ^{t}BuOH (12 mL). The reaction mixture was purged with argon for 5 min and was stirred for 16 h at 120 °C in a pressure tube. After cooling the reaction to RT, Et_2O (100 mL) was added and the formed precipitate was filtered off after centrifuging the mixture (4500 rpm, 5 min). The solvent was removed under reduced pressure and the residue was distilled (b.p. 44 °C / 20 mbar) to give MDO (2.80 g, 24.5 mmol, 28%) as a colourless liquid. ^{1}H NMR (500 MHz, $CDCl_3$, δ/ppm): 1.75 (m, 4H, CH_2) 3.45 (s, 2H, CCH_2), 3.92 (m, 4H, 2 − OCH_2)

The same procedure has been applied for *4,7-dimethyl-2-methylene-1,3-dioxepane (DMMDO)* in an analogue fashion with the following differences:

Acetal intermediate: The starting diol was hexane-2,5-diol (10.0 g, 84.7 mmol, 1.0 eq.). Distillation (b.p. 73 °C / 6 mbar) gave the chlorinated acetal (8.63 g, 48.3 mmol, 57%) as a colourless liquid. ^{1}H NMR (500 MHz, $CDCl_3$, δ/ppm): 1.18–1.29 (m, 6H, CH_3), 1.47–1.90 (m, 4H, CH_2), 3.44/3.45/3.46 (3 t, 2H, CH_2-Cl), 3.74–4.25 (m, 2H, $-OCH_2$), 4.7/ 4.90 /5.02 (t, 1H, OCHO).

Final CKA: Distillation (b.p. 51 °C/ 12 mbar) gave DMMDO (2.40 g, 16.9 mmol, 32%) as a colourless liquid. ^{1}H NMR (500 MHz, $CDCl_3$, δ/ppm): 1.28/1.30 (2 × d, 6H, CH_3), 1.51–1.87 (m, 4H, CH_2-CH2), 3.44 / 3.49 (2 × s, 2H, CCH_2), 3.97–4.07 / 4.19–4.32 (2 × m, 2H, $CHCH_3$).

3.2. 2-methylene-1,3,6-trioxocane (MTC) with the following differences:

Acetal intermediate: The starting diol was Diethylene glycol (1.00 g, 9.40 mmol, 1.0 eq.). Distillation (b.p. 72 °C / 0 mbar) gave the chlorinated acetal (450 mg, 27.0 mmol, 30%) as a colourless liquid which becomes a solid material when stored at 4–8 °C. ^{1}H NMR (500-MHz, $CDCl_3$, δ/ppm): 3.47 (d, 2H, CH_2Cl), 3.66–3.8, 3.9–4.02 (m, 8H, 4 OCH_2), 4.78 (t, 1H, OCHO).

Final CKA: Distillation (b.p. 75 °C / 30 mbar) gave MTC (510 mg, 3.92 mmol, 53%) as a colourless liquid. ^{1}H NMR (500 MHz, $CDCl_3$, δ/ppm): 3.66 (s, 2H, C-CH_2), 3.57–3.77, 4.04–4.06 (m, 8H, OCH_2).

3.3. 5,6-benzyl-2-methylene-1,3-dioxepane (BMDO) with the following differences:

Acetal intermediate: The starting diol was 1,2-Benzenedimethanol. After drying, the solvent was removed under reduced pressure and the residue was recrystallised from cyclohexene to give the chlorinated acetal (1.30 g, 7.02 mmol, 97%) as a white solid. ^{1}H NMR (500 MHz, $CDCl_3$, δ/ppm): 3.67 (d, 2H, CH_2Cl), 4.93 (s, 4H, 2 OCH_2), 5.07 (t, 1H, OCHO), 7.23 (m, 4H, aromatic H).

Final CKA: From the supernatant in Et_2O, the solvent was removed under reduced pressure to give BMDO (1.50 g, 7.80 mmol, 83%) as a pale yellow solid. ^{1}H NMR (500 MHz, $CDCl_3$, δ/ppm): 3.74 (s, 2H, C-CH_2), 5.07 (s, 4H, OCH_2), 7.1–7.28 (m, 4H, aromatic H).

Synthetic procedure using the original method adopted from Bailey et al. [7] In brief, the starting diols (38.0 mmol, i.e. 3.40 mL MDO, 4.70 mL DMMDO, 3.60 mL MTC, 5.20 g BMDO, each corresponding to 1.0 eq.) were mixed with 50 mg Dowex WX8 and chloroacetaldehyde dimethyl acetal (4.70 mL, 41.0 mmol, 1.1 eq.). The mixture was purged with nitrogen for five minutes and heated up to 120 °C under nitrogen gas. The formed methanol was removed by a distillation bridge and reflux condenser. After the calculated amount of methanol has been collected, the reaction was stopped (1 h). The resin was removed by filtration and the products were purified by distillation (for details see cobalt-pathway), except for BMDO which was recrystallised in cyclohexene.

The carbonate route towards DMMDO was published earlier [14] and herein adopted for **MDO**.

Carbonate intermediate: 1,4-Butanediol (1.00 g, 11.1 mmol, 1.0 eq.) was dissolved in DCM (170 mL) and pyridine (7.5 mL) and the reaction mixture was cooled to −20 °C. Triphosgene (5.60 g, 17.0 mmol, 1.5 eq.) was dissolved in DCM (90 mL) and added over 15 min. The cooling bath was removed and the reaction was allowed to warm to RT. After 20 min, the reaction was quenched with sat. *aq.* NH_4Cl. The aqueous phase was extracted with DCM (3x150 mL), washed with brine and dried over $MgSO_4$. Recrystallisation in hexane (2x) yielded MDO-carbonate (760 mg, 6.55 mmol, 59%). ^{1}H NMR (500 MHz, $CDCl_3$, δ/ppm): 4.06–4.14 (m, 4H, $-OCH_2-$), 1.74–1.67 (m, 4H, $-CH_2-CH_2-$).

Final CKA: MDO-carbonate (250 mg, 2.15 mmol, 1.0 eq.) was mixed with a 6 wt% dimethyltitanocene solution (Petasis reagent) in 50% v/v THF/toluene (16.6 mL, 4.31 mmol, 2.0 eq.). The reaction mixture was heated to 65 °C for 20 h and quenched with *n*-hexane (30 mL). The precipitated titanium salt was filtered off and the filtrate was removed under reduced pressure. The crude product was assayed by ^{1}H NMR (peak list see above).

Calculations: DFT-based calculations have been carried out using Gaussian09 [27,28]. Relaxations of the reactants and products as well as the transition state (TS) searches were performed in gas phase. For the polymerisation reaction with two reactants, each reactant was optimised separately (infinite separation). For the calculations, RB3LYP, resp. UB3LYP [29,30] were used as functionals and 6-31G* as basis set [31,32]. These settings for DFT-based calculations were adopted from literature that studied similar radical reactions [33–36] and demonstrate sufficient accuracy for a qualitative description of the activation barriers herein. The imaginary frequencies of the TS search-calculation were analysed using a molecular viewer from Gaussian.

Polymerisations: For heat- and ultrasound-aided polymerisations, the following amounts were used:

MDO (200 mg, 1.75 mmol) with AIBN (3.50 mg, 21.8 μmol;
DMMDO (200 mg, 1.40 mmol) with AIBN (2.87 mg, 17.5 μmol);
BMDO (200 mg, 1.23 mmol) with AIBN (2.46 mg, 15.3 μmol);
MTC (200 mg, 1.50 mmol) with AIBN (3.11 mg, 19.7 μmol)

Thermally initiated polymerisations: CKA (always 200 mg) and AIBN (each 1.25 mol%, weight varies with molecular weight of the monomer, see above) were dissolved in dry toluene (50 μL) in a vial. The mixture was purged with argon for 15 min and was stirred at 85 °C for 24 h under an argon atmosphere. The reaction was cooled to RT and the mixture was dissolved in DCM (50 mL) and dialysed (MWCO 1000 Da) against DCM (300 mL) three times for at least 3 h each. The solvent was removed under reduced pressure to yield the respective polymers.

Ultrasound-aided polymerisations (US-RROP): CKA (always 200 mg) and AIBN (each 1.25 mol%, weight varies with molecular weight of the monomer, see above) were dissolved in dry toluene (50 μL) in a vial. The mixture was purged with argon for 15 min and was stirred at 80 °C (bath temperature) for 3 days under an argon atmosphere in ultrasonic bath. The reaction was cooled to RT and the mixture was dissolved in DCM (50 mL) and dialysed (MWCO 1000 Da) against DCM (300 mL) three times for at least 3 h each. The solvent was removed under reduced pressure to yield the respective polymers.

Photoinitiated polymerisations (photo-RROP) with BME: Photoinitiated experiments were adopted[16,37] and carried out with BME as photoinitiator and a xenon-mercury lamp as a UV light source from *HamamatsuPhotonics UV-Spot LC4* with an output of 140 mW/cm^2 at 365 nm. In a vial, CKA (200–500 mg, see table below) and BME (0.02 eq., see table below) were stirred under UV-irradiation of 365 nm at RT for 24 h (MDO, BMDO) and 48 h (DMMDO, MTC). The crude product was dialysed (MWCO 500 Da) against *aq.* EtOH (15%) three

times for at least 3 h each (see table below). The solvent was removed under reduced pressure to yield the respective polymers.

The following amounts were used:

MDO: 200 mg, 1.74 μmol with BME (7.96 mg, 35.1 μmol) to yield 10.1 mg

BMDO (+50 μL of PhMe): 200 mg, 1.23 mmol with BME (5.58 mg, 24.6 μmol) to yield 23.0 mg

DMMDO: 200 mg, 703 μmol with BME (7.02 mg, 31.0 μmol) to yield 12.6 mg

MTC: 500 mg, 3.84 mmol with BME (17.4 mg, 76.8 μmol) to yield 29.1 mg

Degrees of ring-opening were determined by ^{13}C NMR spectroscopy using an established protocol [16,17,19]. In brief, the carbonate peak around 170 ppm and the acetal peak around 115 ppm were integrated. The relative integral of the carbonate over the combined integrals of both peaks was used to determine the degree of ring-opening.

Amphiphilic block-copolymers were synthesised using a previously published procedure on DMMDO [14], which was equally applied for the other monomers in this work. In brief, the same protocol as for thermally initiated polymerisations was used, but using 15 mg of a PEG_{12}-N = N-PEG_{12} initiator per 200 mg CKA. The initiator was synthesised using the Steglich esterification [38] of 4,4′-(diazene- 1,2-diyl) bis(4-cyanopentanoic acid) with MeO-PEG_{12}-OH using a published procedure [14]. The block-copolymers were purified using dialysis (MWCO 750 Da) against EtOH, exchanging the solvent three times and leaving each batch of solvent for 2 h.

Self-assembly was done using the following procedure: The polymer (2 mg) was dissolved in DCM (1 mL) in a glass vial. The solvent was evaporated under reduced pressure and the surface of the glass was covered in a small film of polymer. PBS (1 mL) was added and the mixture was stirred for two days until further measurements were conducted.

Degradation with esterase from porcine liver was performed on the created self-assemblies based on a previously published procedure [14,16]. In Brief, 2 wt% of esterase in PBS buffer were mixed with the self-assemblies and stirred at 37 °C, while the disassembly process is monitored by DLS as described.

4. Results and discussion

4.1. Monomer synthesis

Following the recent update of the original acetal route towards CKAs, the $CoCl_2$/TMSCl catalytic system (new acetal route) with reduced reaction time and reaction temperature towards was now expanded and optimised. In addition, the new carbonate route towards DMMDO and amine-bearing CKAs *via* a cyclic carbonate intermediate was expanded as well [14,16]. Both new pathways were now applied onto other common CKAs, like 2-methylene-1,3-dioxepane (MDO), 2-methylene-1,3,6-trioxocane (MTC) and 5,6-benzyl-2-methylene-1,3-dioxepane (BMDO) (Figs. 1 and 2). For comparison, all monomers were also synthesised *via* the original acetal route to judge the feasibility fo the new routes.

CKA synthesis *via* the $CoCl_2$/TMSCl catalysed new acetal route was expanded and the necessary cobalt loading was minimised for each monomer. 2 mol% was the minimal catalyst load to reach the acetal precursor of MDO, 4 mol% was the minimum required towards the precursors of DMMDO and BMDO and 8 mol% was the minimal loading to get the precursor of MTC (Fig. 2a). Less cobalt always led to a significant reduction of the yield (see section 1 of the SI). The chlorinated acetal intermediate of BMDO had the highest yield of 97%, whereas those of MDO and DMMDO resulted in acceptable yields of 60% and 57%, respectively. A considerably lower yield of 30% was achieved for the acetal intermediate of MTC (Fig. 2a). Together with the subsequent elimination step, the yields followed a similar trend. BMDO had the highest combined yield of 81%, followed by DMMDO (19%), MDO (17%) and MTC (16%). For MTC the low overall yield was mainly contributed by the relatively low yield in the first step, which could be attributed to an increased ring strain of the eight-membered ring [39]. Low yields for aliphatic seven-membered rings MDO and DMMDO resulted from the low yields in the elimination step (Fig. 2, top), presumably due to occurring side reactions. The adjacent phenyl ring of BMDO is known to stabilise both the chlorinated acetal intermediate [23,40], as well as the final CKA, explaining the high overall yield of this monomer.

These results were compared with those of the original acetal route (Fig. 2) [7,8]. The original protocol included an acidic catalyst and constant removal of methanol by distillation until completion of the reaction. Comparing two Dowex WX catalysts, a cross-linking density of 2% and 8% was tested. The higher cross-linking density led to higher yields and thus, was used for all experiments. Since dealing with acetals, the catalyst was prone to hydrolyse some of the reagent and/or product, inhibiting quantitative reactions. Besides the experimental yields from this study, the results reported in the literature were included in brackets. As for the seven-membered CKAs MDO and DMMDO, the yields of the respective chlorinated acetal intermediates were similar with 64% (68% [7]) and 66% (74% [8]), respectively. Both yields were in the range of those from the new acetal route. The yield of the chlorinated acetal intermediates was 45% for both BMDO (48% [8], 82–86% for Br instead of Cl [15,41]) and MTC (44% for Br instead of Cl [42]). For the synthesis towards BMDO, this yield was considerably lower compared to that of the new pathway (97%), but was higher for the intermediate of MTC (30% yield in the new pathway). Overall, the new acetal route resulted in better or similar yield results for seven-membered chlorinanted acetals, but not for the eight-membered ring towards MTC. Since the new acetal route was performed at RT, it still had an overall advantage over the original acetal route, which was conducted at 120 °C.

Synthesising the CKAs via the carbonate route (Fig. 2b) gave similar yields for the carbonate intermediates of MDO (59%) and DMMDO (66%). No suggested carbonate intermediates could be isolated for BMDO and MTC (Fig. 2b). As for MTC, this was explained by the molecule's high ring strain, which also led to the low yield of the chlorinated acetal intermediate. With respect to BMDO, the reactivity of the OH groups in the starting diol might be too high, promoting the formation of side products rather than the formation of the intended ring structure. The methylenation of the cyclic carbonates of MDO and DMMDO was achieved by using dimethyltitanocene (Petasis reagent), leading to overall yields of 18% and 43%, respectively (Fig. 2b). For MDO, there was no difference compared to the acetal pathway, while the carbonate pathway gave a higher overall yield towards DMMDO. The route *via* a carbonate intermediate was hence less versatile and required an increased synthetic effort (e.g., freshly synthesised Petasis reagent) compared to both acetal routes, rendering it an inferior choice.

4.2. Polymerisation

During polymerisation, CKAs are known to have two pathways as they either open towards the ester or propagate the polymerisation as the closed-ring (ring-opening *vs*. ring-retaining, Fig. 3a). DFT-based calculations for both pathways were performed for all four monomers mentioned above to complement literature data [32]. Since it is a characteristic value, the activation energy (E_A, Fig. 3) for the desired intramolecular ring-opening reaction was compared with the corresponding value for the competing intermolecular ring-retaining reaction (Fig. 3a). E_A of the ring-opening reaction proved to be higher than for the ring-retaining reaction in all instances, ranging from 13.3 kJ/mol for DMMDO over 21.8 kJ/mol for MDO and 31.6 kJ/mol for BMDO to 42.5 kJ/mol for MTC (see Fig. 3b and 3c as well as section 3 of the SI for details). The ring-retaining reaction was hence thermodynamically favoured, but kinetically hampered due to sterical hindrance, leading to degrees of ring-opening of 75–95% in almost all reported examples of

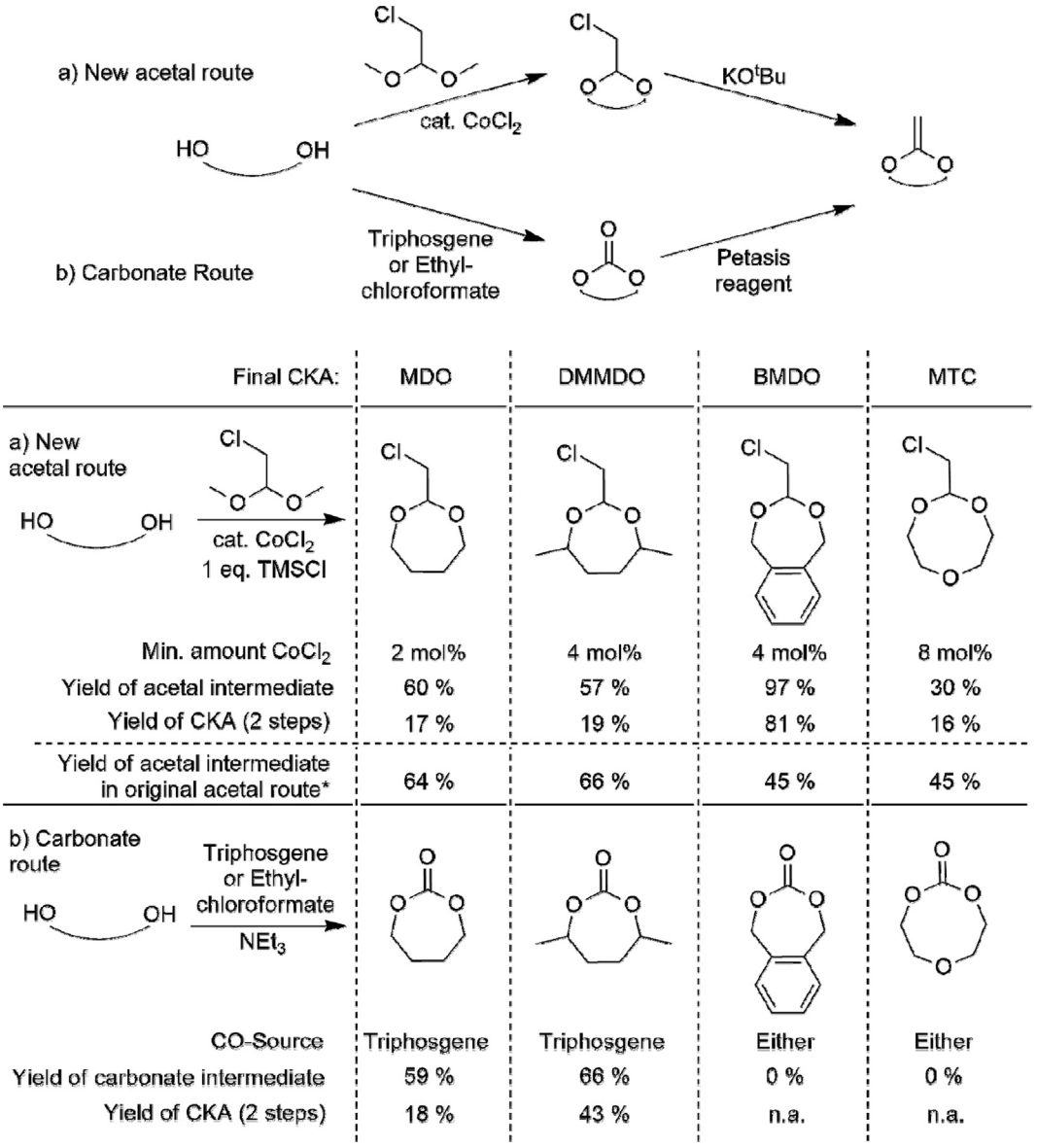

Fig. 2. *Top: Reaction scheme representing the new acetal route and the carbonate route Bottom: a) The diols react towards their corresponding CKAs via their chlorinated acetal intermediates. The table shows the minimum necessary amount of $CoCl_2$, the yield of the acetal and the overall yield towards the final CKA over both steps. *Repeating the synthesis reported by Bailey et al. [7,8] b) The diols react towards their corresponding CKAs via their cyclic carbonate intermediates. The table shows the preferred carbonyl source, the yield of the carbonate and the overall yield towards the final CKA over both steps.*

RROP homopolymers [5,6]. The recently reported amine bearing CKAs *N*-isopropyl-2-methylene-1,3,6-dioxazocane (i-MAC,) and *N*-isopropyl-4,8-dimethyl-2-methylene-1,3,6-dioxazocane (i-DMMAC, see section 3 of the SI for structures) were also addressed to assess the scope of the method [16]. They showed an inverted pattern as the E_A for the ring-retaining reaction was now higher (Fig. 3c, 21.2 kJ/mol (i-MAC) and 66.9 kJ/mol (i-DMMAC). Although the relative difference between activation energies of both pathways provided valuable insights, the exact values had to be treated with caution. This was due to approximations associated with DFT-based calculations (see section 3 of the SI) and because intermolecular reactions are influenced by other parameters than intramolecular reactions.

Following the theoretical discussions, all monomers of this study were subjected to a thermally initiated polymerisation, an ultrasound-aided polymerisation and a photoinitiated polymerisation. All polymerisations were run as homopolymerisations, which was in contrast to the existing literature that mainly covered copolymerisations with vinylic monomers. Thermally initiated polymerisations were the starting point and will be discussed together with ultrasound-aided RROP (US-RROP) below, followed by first experiments on a photo-initiated RROP (photo-RROP). The study focussed on the reached molecular weight as well as on the degree of ring-opening as benchmark characteristics of the final polymer. Both values should be as high as possible. Molecular weights were determined using GPC and degrees of ring-opening were obtained using ^{13}C NMR spectroscopy (see details for each monomer in section 4 of the SI).

Applying ultrasound to the polymerisation (US-RROP) was supposed to overcome the issue of insufficient ring-opening, since this technique is known to promote ring-opening reactions [43,44]. Consequently, applying US-RROP tripled the molecular weight compared to thermally initiated polymerisation for MDO (16400 from 5000 g/mol) and DMMDO (7800 from 2900 g/mol). BMDO (500 g/mol for both) and MTC (5300 from 5200 g/mol) gave no higher molecular weights (Fig. 4, Pathway b). Only oligomers were formed for BMDO due to the strong stabilising effect of the benzyl ring. All polymers showed the surprising effect that the degree of ring-opening decreased in US-RROP. MDO only

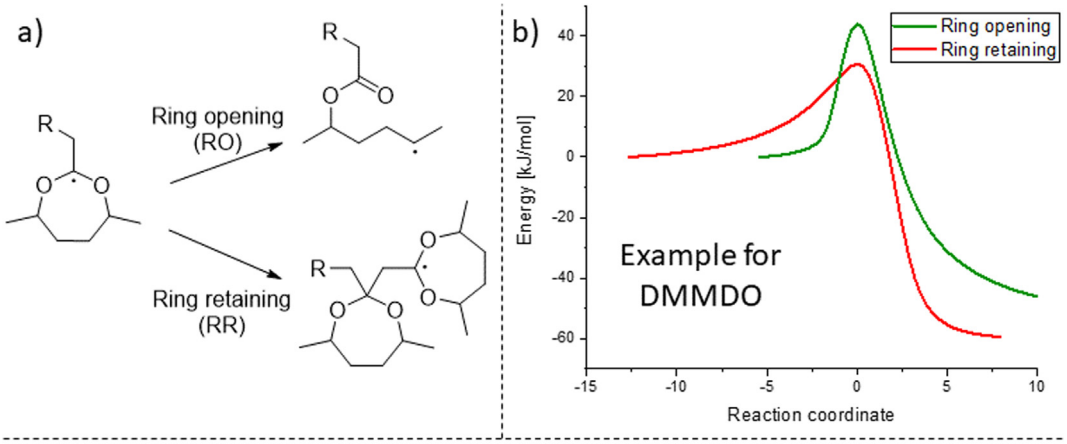

c)

Monomer	MDO	DMMDO	BMDO	MTC	i-MAC	i-DMMAC
$\Delta E_A = E_A(RO) - E_A(RR)$	21.8 kJ/mol	13.3 kJ/mol	31.6 kJ/mol	42.5 kJ/mol	-21.2 kJ/mol	-66.9 kJ/mol

Fig. 3. a) CKAs can propagate the radical in two ways – they either open the ring (Ring-Opening) or retain the ring structure (Ring Radical). b) Both reaction pathways have been plotted for DMMDO using DFT-based calculations. c) The differences in activation energies are noted in kJ/mol . The structures of the amine-bearing monomers i-MAC and i-DMMAC are shown in section 3 of the SI.

gave 89% ring-opening in comparison to 97% in pure thermal initiation, but was still the highest value. The values for DMMDO dropped from 75% to 60% and for MTC from 80% to 61%. For BMDO the value remained low (46% ring-opening in comparison to 45%), but this had to be treated with caution due to the very low molecular weight of polymerised BMDO. Since BMDO is otherwise known to have a high degree of ring opening of 90% or higher [40,45,46], the low molecular weights of this study were a likely reason for the lack of ring-opening. It could be hypothesised that US acted as an additional energy input and promoted the ring-retaining reaction for the polymerising CKAs MDO, DMMDO and MTC. This could be rationalised since the ring-retaining reaction is slowed down by steric hindrance of the triple-substituted carbon atom bearing the radical sustaining the reaction in the ring-retaining pathway. When more energy was inserted into the system, the

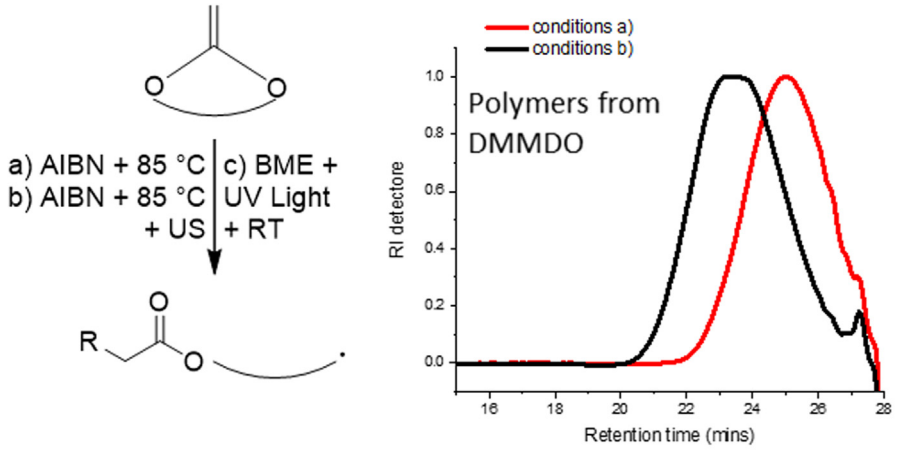

Fig. 4. GPC traces of the polymerisation of DMMDO using heat (red) and ultrasound (black). The table below shows the molecular weights after purification and in brackets the degrees of ring-opening for all three methods of activation for all monomers examined (Thermal, US-RROP and photo-RROP). Dispersities were 1.8–2.2 for all polymerisations. *reaction time 48 h instead of 24 h to reach complete monomer conversion as for all other experiments.

Molar Masses (%age ring opening)

Conditions / Monomer	**MDO** (in g/mol)	**DMMDO** (in g/mol)	**BMDO** (in g/mol)	**MTC** (in g/mol)
a) Thermally initiated	5000 (97 %)	2900 (75 %)	500 (45 %)	5200 (80 %)
b) Thermally initiated + US	16400 (89 %)	7800 (60 %)	500 (46 %)	5300 (61 %)
c) Photo-RROP	3500 * (88 %)	3300 (67 %)	600 (76 %)	19600 * (94 %)

molecules exhibited a higher random movement that promoted reactions with a larger steric hindrance. Observing a larger degree of ring-retention, hence a smaller degree of ring-opening, was the resulting consequence despite the difference in activation energy discussed earlier. Thus, these results suggested that US-RROP favoured the thermodynamic product, which was kinetically hindered using thermal initiation. Altogether, the lower degree of ring-opening was a setback, but the higher molecular weights achieved for MDO and BMDO are a motivating basis for more detailed studies in the future.

Photoinitiated polymerisation (photo-RROP) was known to promote RROP [37] and has only been reported on RROP of pH-sensitive CKAs [16]. Using BME as photoinitiator, the monomers of this study were polymerised using photo-RROP (Fig. 4, pathway c). As in previous polymerisations, BMDO only yielded an oligomer. The molecular weights of the polymers obtained from the other monomers differed for the seven- and eight-membered CKAs. Photo-RROP of MDO yielded a polyester of lower molecular weight than thermally initiated polymerisation (3500 g/mol compared to 5000 g/mol) and DMMDO yielded a polyester of only slightly higher molecular weight (3300 g/mol compared to 2900 g/mol). MTC was a distinct exception, since poly-MTC grew to a polyester of 19600 g/mol after 48 h, *i.e.*, almost four times higher than the molecular weight reached with conventional polymerisation (5200 g/mol). Polyesters from DMMDO and MDO both showed a lower degree of ring-opening compared to conventional polymerisation with 67% and 88% ring-opening, respectively (Fig. 4, pathway c). MTC showed a degree of ring-opening of 94%, indicating that photo-RROP increased both the molecular weight and the degree of ring-opening for this eight-membered CKA. These first results on photo-RROP suggested that the reaction was running under kinetic control, hampering the thermodynamically favoured, yet sterically hindered ring-retaining product. Altogether the ring-opening rates for homopolymerisations using photo-RROP and US-RROP were lower than for copolymers with vinylic monomers using heat initiated RROP in all cases as these reactions can reach full ring-opening [5,9,20].

Thermograms were recorded for all polymers and revealed a very similar behaviour for polymers from MDO, DMMDO and MTC with respect to their glass transition temperatures (T_g's). The methyl side groups of poly-DMMDO (or poly(dimethylcaprolactone (PdmCL)) induced mobility at the lowest temperature, giving this polymer a T_g of −71.2 °C. Poly-MDO (or poly(caprolactone) (PCL)) followed with a T_g of −65.2 °C and poly-MTC showed a similar T_g of −63.6 °C (Fig. 5). The oligomers from BMDO showed a higher T_g of −19.4 °C which could be attributed to the phenyl ring in the structure. It has to be noted that the low degree of polymerisation suggested that the T_g of oligo-BMDO was still dependent on the molecular weight. Poly-MDO showed a notable exception with a melting temperature (T_m) of −8.3 °C (onset, Fig. 5), exposing a semi-crystalline behaviour for this polymer. This agreed with earlier reports where poly-MDO was described as a branched version of PCL, a semi crystalline polymer [5,25]. However, Agarwal *et al.* reported no T_m due to the large degree of branching in poly-MDO. The measured T_m in the present study suggested the presence a semi-crystalline polymer originating from linear segments within the polymer. The higher reaction temperature (85 °C instead of 70 °C) might have led to decreased branching since an increased reactivity of MDO may have reduced the occurrence of side reactions. including branching. Another possible reason is that the use of small amounts of toluene may have supressed H-transfer as a side reaction and promoted the formation of linear polymers [23]. The originally small crystallinity of poly-MDO was significantly enhanced when US-RROP was used. Together with the higher molecular weight reached with US-RROP, these findings implied a larger amount of crystallites (larger melting peak) but not a larger size of them, since the melting temperature did not increase. The cooling curves (see section 5 of the SI) reflected the glass transition temperatures in a similar manner. Exothermal pre-crystallisation peaks were detected in the heating curves, but no crystallisation peaks were detected upon cooling, which could be attributed to the faster cooling rate.

4.3. Nanoparticle formation and degradation

The great strength of RROP of CKAs is that it produces biodegradable polyesters *via* a radical polymerisation. Biodegradation is a key characteristic for drug-delivery systems from polymeric self-assemblies. Amphiphilic block-copolymers, capable of undergoing self-assembly, were prepared from all four monomers in this study. Similar to previous reports, the amphiphilic block-copolymers were obtained using a macroinitiator based on the hydrophilic poly(ethylene glycol) (PEG) [14,16]. PEG-P(BMDO) did not self-assemble into nanoparticles, which could be attributed to the phenyl group in BMDO as it is already known for the phenyl group in polystyrene [47]. All other block-copolymers self-assembled into nanoparticles of 30 nm in radius (see section 6 of the SI). Biodegradation of those nanoparticles using esterase from porcine liver was followed with the count rate of DLS, following an established protocol [14,16,48]. All degradation patterns followed the

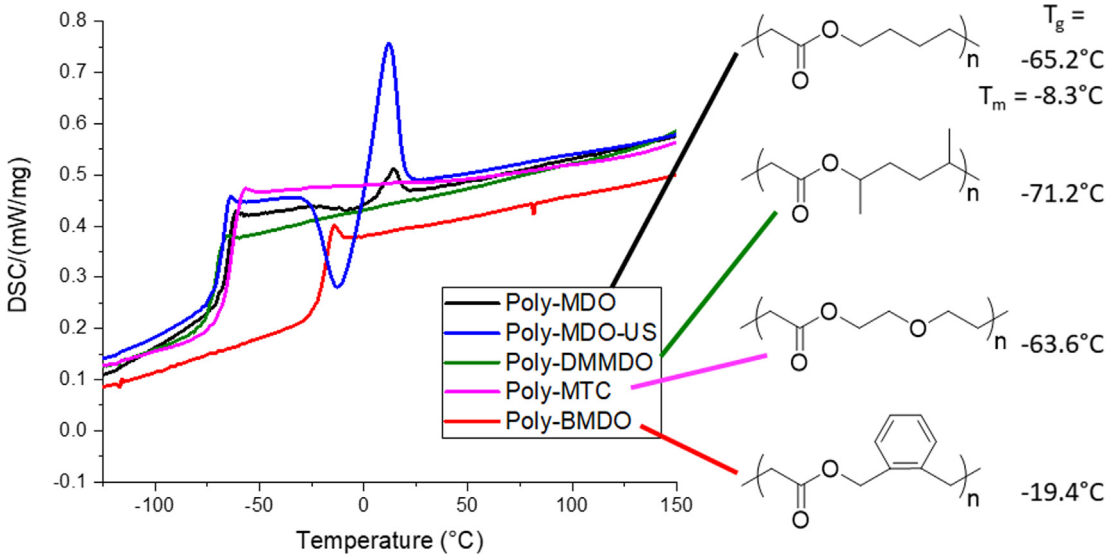

Fig. 5. Thermograms of polymerised MDO, DMMDO, BMDO and MTC (thermal initiation) and their corresponding glass transition and melting temperatures. All show glass transition temperatures. Melting temperatures were detected for polymerised MDO from thermal initiation as well as from US-RROP.

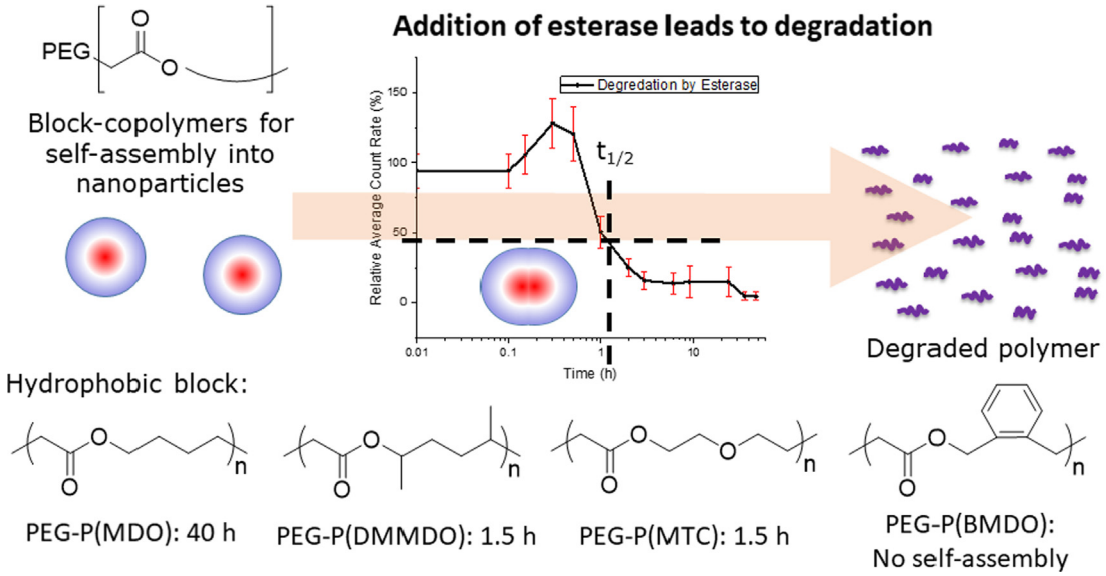

Fig. 6. All monomers were transformed into block-copolymers with PEG and their degradation behaviour examined with esterase from porcine liver. 50% of the original scattering intensity marked the half-life point ($t_{1/2}$) and is noted underneath the corresponding polyesters. PEG-PBMDO did not self-assemble.

same trend, which was reported previously on other systems [14,16]. After an initial spike in the count rate caused by initial agglomeration, the nanoparticles degraded completely (Fig. 6). In order to compare the degradation behaviour, the half-life was defined as the time point when 50% of the original value of the count rate was reached (see section 6 of the SI). Nanoparticles based on totally amorphous poly-DMMDO and poly-MTC both exhibited half-life times of 1.5 h. Nanoparticles based on the semi-crystalline poly-MDO on the other hand, showed a half-life of 40 h (Fig. 6). These results suggested that the semi-crystallinity of poly-MDO significantly prolonged the half-life time of nanoparticles from this polymer.

5. Conclusions

Our study took a thorough look into popular monomers for radical ring-opening polymerisation, namely MDO, DMMDO, BMDO and MTC. All of these monomers proved to be accessible *via* the cobalt-catalysed new acetal route and MDO was also accessible *via* the carbonate route (in addition to the previously reported DMMDO) [14,16]. In terms of their polymerisations, DFT-based calculations showed that the ring-opening reaction had a higher activation energy than the side-reaction of the closed ring propagating reaction. Interestingly, the eight-membered ring (MTC) showed a higher activation energy than CKAs with seven-membered rings (MDO and derivatives). Comparing these aliphatic CKAs to ones bearing tertiary amines, it has been shown that i-MAC and i-DMMAC had lower activation energies for the ring-opening reaction. However, it was not fully resolved how these differences translated into the observed varying degrees of ring opening, motivating further research. Polymerising the CKAs showed that thermally initiated RROP led to the highest degree of ring-opening and US-RROP to the highest molar masses for seven-membered rings, while photo-RROP gave the highest degree of ring-opening and molar mass for the eight-membered ring. BMDO failed to homopolymerise under all investigated conditions. Photo-RROP and US-RROP proved to be interesting candidates sparking an interest into more detailed studies into these new ways to perform RROP. Thermal analyses of the polymers revealed a previously unknown semi-crystallinity of polymerised MDO, which enhanced greatly after US-RROP. The polymers generally showed low T_g's of −71 to −63 °C, where the phenyl ring of BMDO led to an increased T_g of −19.4 °C for the produced oligomers. Apart from BMDO, all polyesters from the CKAs were used as hydrophobic blocks in self-assembling block-copolymers. The resulting nanoparticles proved to be biodegradable by esterase. The non-crystalline polyesters from DMMDO and MTC exhibited a half-life of 1.5 h, while the semi-crystalline polyester from MDO exhibited a half-life of 40 h. Altogether, the results contributed to a deeper insight into structure–property connections for polyesters from RROP and helped to get a better understanding of the reaction.

6. Data availability statement

The raw/processed data required to reproduce these findings cannot be shared at this time as the data also forms part of an ongoing study.

CRediT authorship contribution statement

Jenny Folini: Methodology, Investigation, Data curation, Writing - original draft, Writing - review & editing. **Wigdan Murad:** Methodology, Investigation, Data curation, Visualization. **Fabian Mehner:** Validation, Investigation, Writing - original draft, Writing - review & editing. **Wolfgang Meier:** Conceptualization, Resources, Data curation, Supervision, Project administration, Funding acquisition. **Jens Gaitzsch:** Conceptualization, Methodology, Formal analysis, Resources, Writing - original draft, Writing - review & editing, Visualization, Supervision, Project administration, Funding acquisition.

Declaration of Competing Interest

There are no conflicts to declare.

Acknowledgements

Financial support of the Novartis-University of Basel Fellowship for Excellence in Life Sciences for J.G. and from the Swiss National Science Foundation (SNSF) in light of the National Centre for Competence in Research for Molecular Systems Engineering (NCCR-MSE) is gratefully acknowledged. The authors thank S. Heinen and A. v. Lilienfeld (University of Basel) for their support with the calculations of the activation energies.

References

[1] T. Iwata, Angew. Chem., Int. Ed. 54 (2015) 3210–3215.
[2] T.P. Haider, C. Völker, J. Kramm, K. Landfester, F.R. Wurm, Angew. Chem., Int. Ed. 58 (2019) 50–62.
[3] O. Nuyken, S.D. Pask, Polymers 5 (2013) 361–403.
[4] S.P. Hsu, I.M. Chu, J.D. Yang, J. Appl. Polym. Sci. 125 (2012) 133–144.
[5] A. Tardy, J. Nicolas, D. Gigmes, C. Lefay, Y. Guillaneuf, Chem. Rev. 117 (2017) 1319–1406.
[6] S. Agarwal, Polym. Chem. 1 (2010) 953–964.
[7] W.J. Bailey, Z. Ni, S.R. Wu, J. Polym. Sci., Part A: Polym. Chem. 20 (1982) 3021–3030.
[8] W.J. Bailey, Z. Ni, S.R. Wu, Macromolecules 15 (1982) 711–714.
[9] M.R. Hill, E. Guégain, J. Tran, C.A. Figg, A.C. Turner, J. Nicolas, B.S. Sumerlin, ACS Macro Lett. 6 (2017) 1071–1077.
[10] P. T. Anastas and J. C. Warner, Oxford University Press: Oxford, 1998.
[11] W.J. Bailey, S.R. Wu, Z.D. Ni, Journal of Macromolecular Science-Chemistry A18 (1982) 973–986.
[12] W.J. Bailey, S.R. Wu, Z. Ni, Macromol. Chem. Phys. 183 (1982) 1913–1920.
[13] S. Jin, K.E. Gonsalves, Macromolecules 30 (1997) 3104–3106.
[14] J. Gaitzsch, P.C. Welsch, J. Folini, C.-A. Schoenenberger, J.C. Anderson, W.P. Meier, Eur. Polym. J. 101 (2018) 113–119.
[15] S. Ganda, Y. Jiang, D.S. Thomas, J. Eliezar, M.H. Stenzel, Macromolecules 49 (2016) 4136–4146.
[16] J. Folini, C.-H. Huang, J.C. Anderson, W. Meier, J. Gaitzsch, Polym. Chem. 10 (2019) 5285–5288.
[17] M.R. Hill, T. Kubo, S.L. Goodrich, C.A. Figg, B.S. Sumerlin, Macromolecules 51 (2018) 5079–5084.
[18] J.Y. Yuan, C.Y. Pan, Eur. Polym. J. 38 (2002) 2069–2076.
[19] G.G. Hedir, C.A. Bell, R.K. O'Reilly, A.P. Dove, Biomacromolecules 16 (2015) 2049–2058.
[20] C.A. Bell, G.G. Hedir, R.K. O'Reilly, A.P. Dove, Polym. Chem. 6 (2015) 7447–7454.
[21] J. Tran, E. Guegain, N. Ibrahim, S. Harrisson, J. Nicolas, Polym. Chem. 7 (2016) 4427–4435.
[22] G. Hedir, C. Stubbs, P. Aston, A.P. Dove, M.I. Gibson, ACS Macro Lett. 6 (2017) 1404–1408.
[23] A. Tardy, J.C. Honore, D. Siri, D. Siri, D. Gigmes, C. Lefay, Y. Guillaneuf, Polym. Chem. 8 (2017) 5139–5147.
[24] E. Guégain, C. Zhu, E. Giovanardi, J. Nicolas, Macromolecules 52 (2019) 3612–3624.
[25] S. Agarwal, C. Speyerer, Polymer 51 (2010) 1024–1032.
[26] J. Tran, T. Pesenti, J. Cressonnier, C. Lefay, D. Gigmes, Y. Guillaneuf, J. Nicolas, Biomacromolecules 20 (2019) 305–317.
[27] P. Hohenberg, W. Kohn, Physical Review 136 (1964) B864–B871.
[28] W. Kohn, L.J. Sham, Physical Review 140 (1965) A1133–A1138.
[29] A.D. Becke, The Journal of Chemical Physics 98 (1993) 5648–5652.
[30] C. Lee, W. Yang, R.G. Parr, Physical Review B 37 (1988) 785–789.
[31] T. Clark, J. Chandrasekhar, G.W. Spitznagel, P.V.R. Schleyer, J. Comput. Chem. 4 (1983) 294–301.
[32] B. Ochiai, T. Endo, J. Polym. Sci., Part A: Polym. Chem. 45 (2007) 2827–2834.
[33] Z. Velkov, E. Balabanova, A. Tadjer, Journal of Molecular Structure: THEOCHEM 821 (2007) 133–138.
[34] E.E. Greenwald, S.W. North, Y. Georgievskii, S.J. Klippenstein, The Journal of Physical Chemistry A 109 (2005) 6031–6044.
[35] J.P. Senosiain, S.J. Klippenstein, J.A. Miller, The Journal of Physical Chemistry A 110 (2006) 6960–6970.
[36] J. Lalevée, B. Graff, X. Allonas, J.P. Fouassier, The Journal of Physical Chemistry A 111 (2007) 6991–6998.
[37] I. Cho, B.G. Kim, Y.C. Park, C.B. Kim, M.S. Gong, Makromolekulare Chemie-Rapid Communications 12 (1991) 141–146.
[38] B. Neises, W. Steglich, Angewandte Chemie International Edition in English 17 (1978) 522–524.
[39] C. Galli, L. Mandolini, Eur. J. Org. Chem. 2000 (2000) 3117–3125.
[40] J.Y. Huang, R. Gil, K. Matyjaszewski, Polymer 46 (2005) 11698–11706.
[41] B. Iyisan, A.C. Siedel, H. Gumz, M. Yassin, J. Kluge, J. Gaitzsch, P. Formanek, S. Moreno, B. Voit, D. Appelhans, Macromol. Rapid Commun. 38 (2017) 1700486.
[42] J. Undin, P. Plikk, A. Finne-Wistrand, A.C. Albertsson, J. Polym. Sci., Part A: Polym. Chem. 48 (2010) 4965–4973.
[43] T.J. Mason, Chem. Soc. Rev. 26 (1997) 443–451.
[44] R. Cella, H.A. Stefani, Tetrahedron 65 (2009) 2619–2641.
[45] A. Tardy, V. Delplace, D. Siri, C. Lefay, S. Harrisson, B.D.A. Pereira, L. Charles, D. Gigmes, J. Nicolas, Y. Guillaneuf, Polym. Chem. 4 (2013) 4776–4787.
[46] J.Y. Yuan, C.Y. Pan, Eur. Polym. J. 38 (2002) 1565–1571.
[47] J. Gaitzsch, X. Huang, B. Voit, Chem. Rev. 116 (2016) 1053–1093.
[48] Y. Zhu, A. Poma, L. Rizzello, V.M. Gouveia, L. Ruiz-Perez, G. Battaglia, C.K. Williams, Angew. Chem. 131 (2019) 4629–4634.